

Antimicrobial activity of electrospun polyurethane nanofibers containing composite materials

Rajkumar Nirmala*, Duraisamy Kalpana**, Rangaswamy Navamathavan***, Mira Park*,
Hak Yong Kim*,†, and Soo-Jin Park****,†

*Department of Organic Materials and Fiber Engineering, Chonbuk National University, Jeonju 561-756, Korea

**Department of Forest Science and Technology, Institute of Agricultural Science and Technology,
Chonbuk National University, Jeonju 561-756, Korea

***School of Advanced Materials Engineering, Chonbuk National University, Jeonju 561-756, Korea

****Department of Chemistry, Inha University, Nam-gu, Incheon 402-751, Korea

(Received 12 August 2013 • accepted 27 November 2013)

Abstract—We report on the preparation and characterization of electrospun polyurethane nanofibers containing silver, cactus, rosin and *Scutellariae Radix*. The utilized polyurethane nanofibers containing different composite materials were prepared by a simple dip coating method. The morphology, structure and thermal characteristics of as-prepared composite nanofibers were studied by scanning electron microscopy, X-ray diffraction, Fourier transform infrared, Raman spectroscopy and thermogravimetric analysis. The antimicrobial activity of the composite nanofibers was tested against two common food borne pathogenic bacteria, *Staphylococcus aureus* and *Escherichia coli*, by the minimum inhibitory concentration method. Our results demonstrated that more pronounced antimicrobial activities were observed for the composite nanofibers. Overall, the fabrication of cheap, stable and effective material with excellent antimicrobial activity can be utilized to inhibit the microbial growth associated with food stuff.

Keywords: Electrospinning, Composite Nanofibers, Antimicrobial

INTRODUCTION

Electrospinning is a technique used in materials engineering which recently has significance importance in several areas of application of polymeric materials [1-4]. This technique helps to obtain fibers with diameters in the nanometer range capable of forming a layer with excellent characteristics such as toughness, strength and flexibility. These properties make nanofibers suitable for the creation of numerous technologically advanced products such as for drug delivery, wound dressings, scaffolds and filtration [5-10]. An electrospinning system consists of a polymer solution contained in a syringe with a connected power source. The polymer solution is usually provided a charge using a high voltage power source. The electric field draws this droplet into a structure called a Taylor cone. If the viscosity and surface tension of the solution are appropriately reached, polymer drops break up and a stable jet is formed [11,12].

Antimicrobial polymers have many applications in medical and packaging industries; however, research in natural antimicrobial still has a limited field. In this scope, natural antimicrobial substances exist in animals and plants where they evolved as host defense mechanisms. In this connection, polymers due to their intrinsic properties are extensively and efficiently employed in all of these fields. Therefore, the use of polymeric materials with antimicrobial properties has gained increasing interest from both the academic and industrial point of view. Polymers can act as matrix of the materials holding

the antimicrobial agents. In particular, polyurethane (PU) is a thermoplastic, biodegradable, biocompatible polymer with excellent mechanical and physical properties [13-15]. PU is becoming increasingly important because it is a candidate for different applications such as adhesives, additives, resins, catalysts and in the biomedical field [16-19]. For these merits, PU has been found to be a very promising material of interest. The properties of PU can be adjusted in desired ways according to their requirements [20-22]. Incorporation of biological macromolecules into PU nanofibers has attracted a great deal of attention in biomedical applications because the resulting fibers can have very strong antimicrobial activity. Such kinds of materials can have much improved properties in terms of thermal stability, flexibility and solubility with that of the pristine PU. Herein, we for the first time report on the incorporation of a variety of composites such as silver nitrate, rosin, cactus and *Scutellariae Radix* into electrospun PU nanofibers by using dip coating method.

Rosin is an abundantly available natural material composed of ca. 90% acidic and ca. 10% neutral compounds. The acidic components, rosin acids, are also a mixture mainly consisting of isomeric abietic-type acids (40-60%) and pimaric-type acids (9-27%) on the basis of total rosin weight [23]. Rosin is a natural polymer obtained from pine trees, and its derivatives have attracted much interest in the field of pharmaceutical applications due to their characteristic properties such as biocompatibility, biodegradability and low cost [24-28]. Rosin and its derivatives are traditionally used in adhesive paciers, vanishes, and other niche applications. Baicalein (5,6,7-trihydroxyflavone) and wogonin (5,7-dihydroxy-8-methoxy flavones), which are the aglycones of baicalin (baicalein 7-O-glucuronide) and wogonoside (wogonin 7-O-glucuronide), respectively, are major

*To whom correspondence should be addressed.

E-mail: khy@jbnu.ac.kr, sjpark@inha.ac.kr

Copyright by The Korean Institute of Chemical Engineers.

effective flavones in dried roots of *Scutellaria baicalensis* Georgi [29,30]. They are widely used in traditional Chinese medicine to treat inflammation, fever, jaundice, hypertension, tumors and diarrhea [31-34]. Cactus has received a great degree of attention because it contains many nutritive and medicinal components such as protein amylose, malic acid, rosin, vitamin and cellulose [35,36]. Incorporating biologically active substance in the PU nanofibers has received a great deal of attention in biomedical applications because the resulting fibers have superior antimicrobial activity. Such kinds of composite nanofiber materials can have much improved properties in terms of thermal stability, flexibility and solubility with that of the pristine PU nanofibers.

We prepared PU nanofibers by using electrospinning. The as-spun PU nanofibers were dip-coated with silver, cactus, rosin and *Scutellariae Radix* to obtain composite nanofibers. The resultant PU composite nanofibers were analyzed by scanning electron microscopy (SEM), X-ray diffraction (XRD), Fourier transform infrared spectroscopy (FT-IR), Raman spectroscopy, and thermogravimetric analysis (TGA). The antimicrobial activity of the pristine and PU nanofibers containing composite materials such as silver, cactus, rosin and *Scutellariae Radix* was tested against two common food borne pathogenic bacteria namely, *Staphylococcus aureus* (*S. aureus*) and *Escherichia coli* (*E. coli*) by minimum inhibitory concentration (MIC) method.

EXPERIMENTAL

1. Materials

Polyurethane (PU, Mw=110,000) and silver nitrate (AgNO_3) were purchased from Cardio Tech, Japan. THF and N,N-dimethylformamide (DMF) (analytical grade, Showa, Japan) were used as solvents without further purification. Rosin, cactus, *Scutellariae Radix* (SR, Baicalein 33.0%, Baicalin 32.8%) (A gift from Healthcare Center, Chonbuk National University, Jeonju, South Korea) were used to obtain composite nanofibers.

S. aureus (KCCM 11256) and *E. coli* (KCCM 11234), were purchased from Korean Culture Center of Microorganisms (KCCM). These pathogenic microorganisms were used as the model bacteria for the disc diffusion susceptibility test. For the antimicrobial activity measurement, Mueller-Hinton broth (MHB) & Mueller-Hinton agar (MHA) (Difco, Sparks, MD, USA) were used.

2. Electrospinning of Polyurethane Nanofibers

PU solution with 10 wt% was prepared by dissolving in the solvents of THF and DMF with the ratio of 1 : 1. After that, the polymer solution was loaded into a 5 ml plastic syringe with 1 mm diameter wire needle on syringe pump (KD scientific Co., USA) with a flow rate of 1 $\mu\text{L}/\text{min}$. A high voltage power supply (CPS-60 K02V1, Chungpa EMT, South Korea) of 15 kV to the syringe micro-tip was supplied to electrospin the nanofibers. The tip-to-collector distance was kept at 15 cm. During electrospinning, the drum was rotated at a constant speed by a DC motor to collect the developing nanofibers. Then the nanofibers were vacuum dried and utilized for obtaining composite nanofibers.

3. Preparation of PU Composite Nanofibers

For preparing PU composite nanofibers, AgNO_3 (0.2 mol/L), rosin (5%), cactus (5%), *Scutellariae Radix* (5%) were individually dissolved in DMF solution. The respective solutions were vigorously

stirred for 3 h at room temperature to obtain a homogeneous mixture. Then the solution was gently poured into a Petri dish containing PU nanofibers. Dip coating was performed to obtain the composite nanofibers. The contents were shaken gently to prepare uniform coating of entities on the PU nanofibers. Five different types of nanofiber mats were prepared and labeled: (1) pristine PU (PU), (2) PU with AgNO_3 (PU/Ag), (3) PU with cactus (PU/C), (4) PU with rosin (PU/R) and (5) PU with *Scutellariae Radix* (PU/SR). Careful washing of the nanofiber mat was maintained for 12 h at room temperature. The nanofiber mats were rinsed by ethanol 3 times and dried at 25 °C under vacuum condition to evaporate the residual solvent from the composite nanofiber mats. The resultant PU, PU/Ag, PU/C, PU/R and PU/SR composite nanofibers were utilized for the further characterizations.

4. Characterizations

The morphology of the PU composite nanofibers was observed by scanning electron microscopy (SEM, Hitachi S-7400, Hitachi, Japan). Structural characterization was carried out by X-ray diffraction (XRD) in a Rigaku X-ray diffractometer operated with Cu $\text{K}\alpha$ radiation ($\lambda=1.540 \text{ \AA}$). The bonding configurations of the samples were characterized by Fourier transform infrared (FT-IR) and Raman spectroscopy. Thermogravimetric analysis (TGA, Perkin-Elmer, USA) was carried out for the thin films under nitrogen ambient with a flow rate of 20 mL/min. The samples were heated from 30 to 800 °C at a rate of 10 °C/min.

5. Antimicrobial Activity by the Disc Diffusion Susceptibility Test

The disc diffusion susceptibility test for *S. aureus* and *E. coli* was performed on the MHA plate at the incubation temperature of 37 °C. The MHB containing 1.5×10^6 colony-forming units (cfu) of bacteria were used for the lawn culture. The PU composite nanofibers were cut into 6 mm diameter discs. Then, each bacterium was lawn cultured on the MHA Petri plate by using a sterile cotton swab. The ultraviolet sterilized PU composite nanofiber discs were kept at uniform distance and then incubated overnight at 37 °C. The zone of inhibition was observed after 24 h of incubation and the diameter of the zone was measured.

RESULTS AND DISCUSSION

Fig. 1(a)-1(e) shows the SEM images of the as-obtained pristine PU and PU composite nanofibers. The pristine PU nanofibers are smooth and continuous, with diameters in the range of 200-500 nm. The electrospun PU nanofibers are continuous over long distances as shown in Fig. 1(a). Fig. 1(b)-1(e) shows the dip coated composite nanofibers of PU/Ag, PU/C, PU/R and PU/SR, respectively. Significant morphological difference can be observed between the pristine PU and composite PU nanofibers. Fig. 2(b) shows the AgNO_3 particles attached at the periphery of the PU nanofibers. The morphology of the PU composite nanofibers appeared to be bulging due to the dip coating. The diameter of the resultant PU composite nanofibers after dip coating was observed to be slightly larger (about 600-1200 nm) than that of pristine PU nanofibers. As shown in Fig. 1, we successfully obtained PU composite nanofibers.

XRD was used to investigate the phase structures of the PU composite nanofibers. The XRD diffractograms of the pristine PU and PU composite nanofibers are shown in Fig. 2. The XRD data of

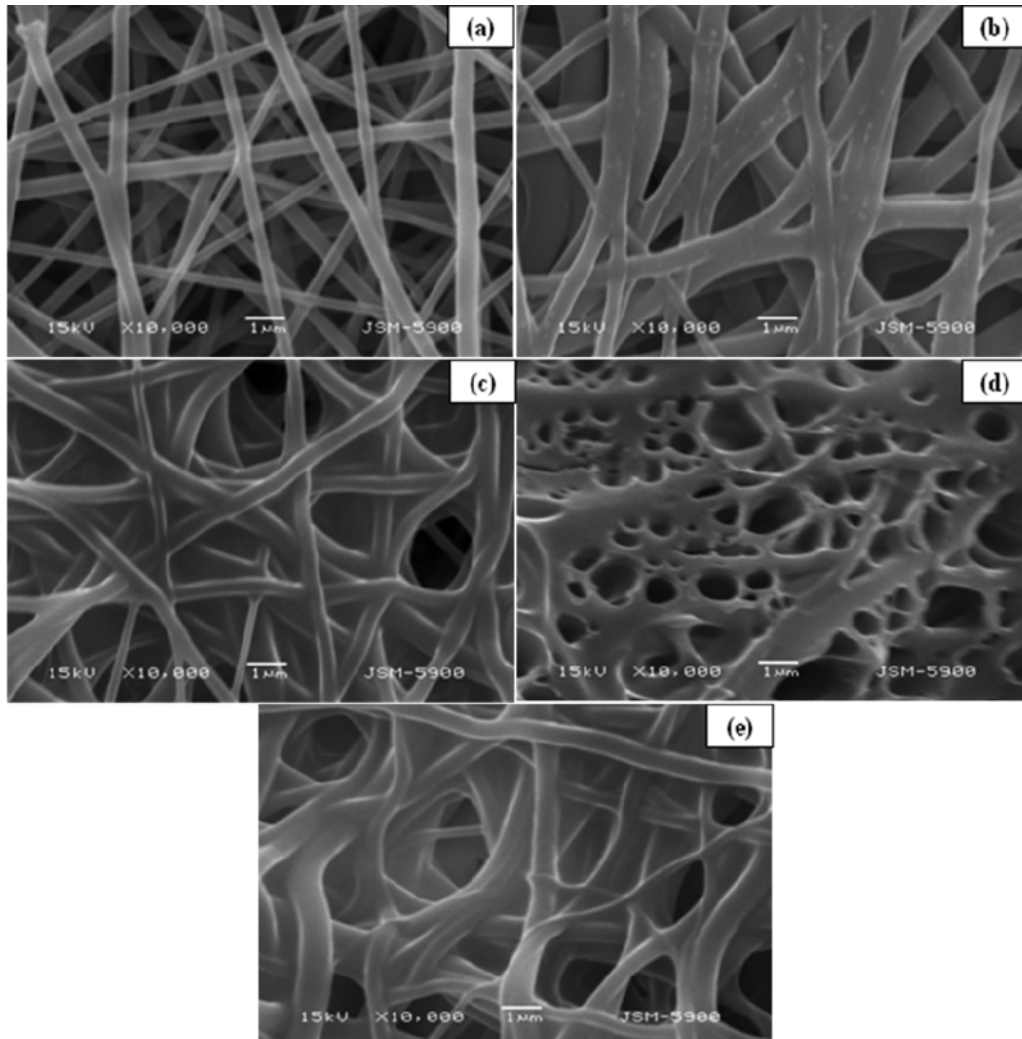


Fig. 1. SEM images of (a) PU, (b) PU/Ag, (c) PU/C, (d) PU/R and (e) PU/SR nanofibers.

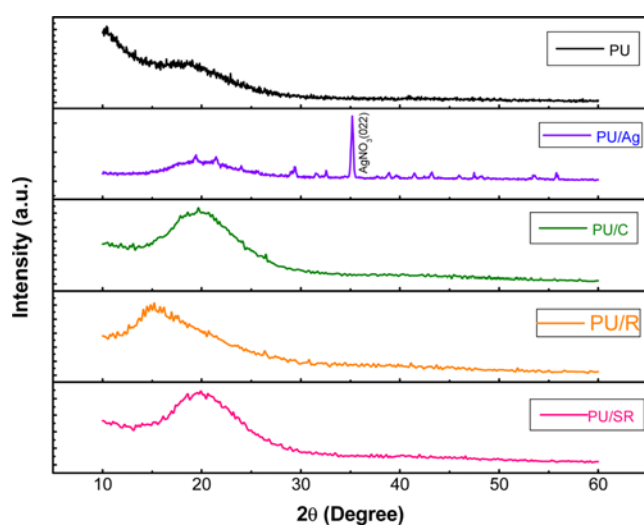


Fig. 2. XRD patterns of pristine PU and PU composite nanofibers.

pristine PU nanofibers exhibited a broad and faint diffraction peak centered at $2\theta=20^\circ$ due to the amorphous nature of fiber structure.

At the same time, no significant changes were observed for the PU/C, PU/R and PU/SR composite nanofibers due to the amorphous form of the constituents. On the other hand, the PU/Ag composite nanofibers exhibited a prominent diffraction peak at 35° corresponding to the (002) plane of AgNO_3 , which is consistent with the JCPDS data (#01-074-4790). The dip coated AgNO_3 did not undergo reduction process to form Ag nanoparticles. No significant diffraction peaks of any other phases or impurities can be detected in the XRD patterns, which indicates the successful formation of PU composite nanofibers.

The structural configurations of PU composite nanofibers were characterized by using FT-IR spectroscopy. Fig. 3 illustrates the FT-IR spectra of the interaction between the PU polymers with AgNO_3 , cactus, rosin, and *Scutellariae Radix* entities. The characteristic transmittance peaks of pristine PU and the PU composite nanofibers were in the range of $500\text{-}1,750\text{ cm}^{-1}$. The various transmittance bands of pristine PU nanofibers were at the wavenumbers of $3,355, 2,955, 1,730, 1,597, 1,288, 1,064$ and 772 cm^{-1} can be assigned to $\nu(\text{N-H})$, $\nu(\text{C-H})$, $\nu(\text{C=O})$, $\nu(\text{C=C})$, $\nu(\text{C-C})$, $\nu(\text{C-O})$, $\nu(\text{C-H})$ stretching modes, respectively [37,38]. The FTIR spectrum of PU/Ag composite nanofibers showed a shifting of hydrogen bonded N-H trans-

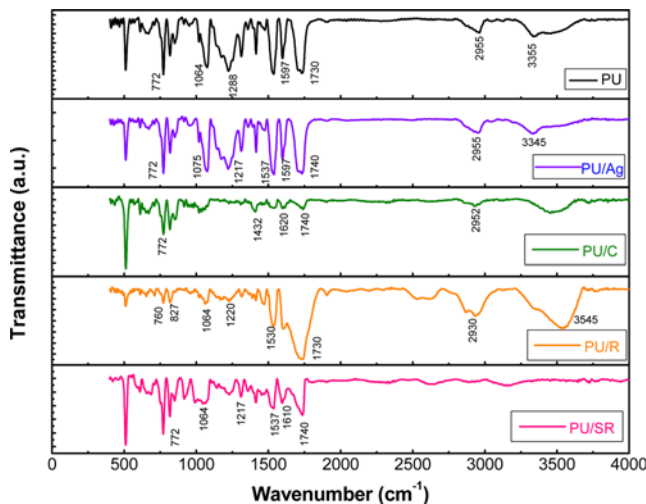


Fig. 3. FT-IR spectra of pristine PU and PU composite nanofibers.

mittance peak toward the lower wavenumber region ($3,345\text{ cm}^{-1}$) with respect to the pristine PU nanofibers owing to the interaction of Ag nanoparticles in the composite nanofibers [39]. As assigned in the FTIR in Fig. 3, the PU/C composite nanofibers exhibited that stretching vibration band $1,620\text{ cm}^{-1}$ was due to asymmetric stretching of the carboxylic C=O double bond. A $1,432\text{ cm}^{-1}$ is of phenolic -OH and -C=O stretching of carboxylates. And peaks in the region of lower wave numbers (under 700 cm^{-1}) appeared as feeble peaks and this could be attributed to the N containing bioligands [40,41]. The PU/R composite nanofibers can be assigned as the following $2,930\text{ cm}^{-1}$ (CH_2 asymmetric vibration); a broad band at $1,730\text{ cm}^{-1}$ (free C-O); $1,530\text{ cm}^{-1}$ (C=O bond); $1,220\text{ cm}^{-1}$ (urethane amide II); $1,064\text{ cm}^{-1}$ (C-O-C stretching of the hard segment); and 827 cm^{-1} (bending vibration) [28]. And, compared with FT-IR spectra of pure PU nanobers, one additional transmittance peak appeared at $1,610\text{ cm}^{-1}$ for the PU/SR composite nanofibers. This result suggested that formation of a hydrogen related bond between PU nanofibers and Scutellariae Radix molecules [33]. A broad transmittance band centered at $3,500\text{ cm}^{-1}$ corresponding to -OH stretching vibra-

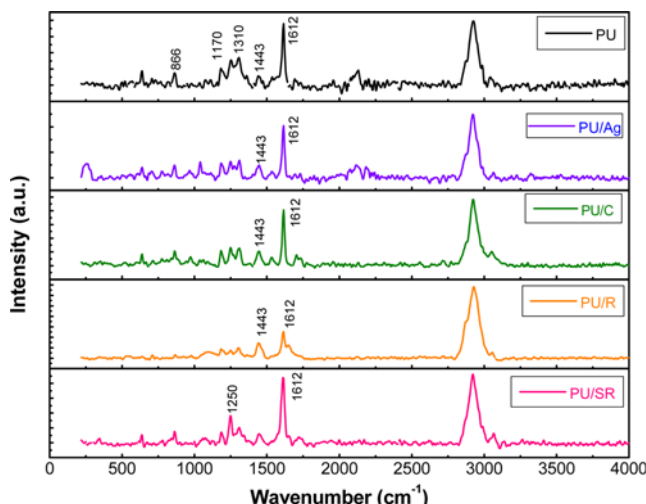


Fig. 3. FT-IR spectra of pristine PU and PU composite nanofibers.

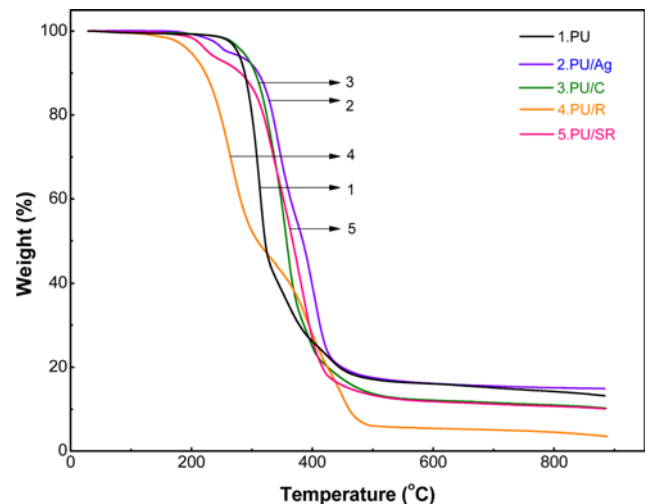


Fig. 5. TGA traces of pristine PU and PU composite nanofibers.

tion was observed. Remarkable changes in the line-shapes and peak intensities between the pristine PU and the PU composite nanofibers were observed. This result implies a pronounced interaction of the molecules in the composite nanofibers.

To further understand the bonding structure of the PU composite nanofibers, we performed Raman spectroscopy. Fig. 4 shows the Raman spectra of the pristine PU and PU composite nanofibers. As observed, significant vibration peaks at $1,200$ and $1,600\text{ cm}^{-1}$ were attributed to the E_g and E_g modes of PU composite nanofibers. Raman peaks were at $866, 1,170, 1,310, 1,443$, and $1,612\text{ cm}^{-1}$ which are attributed the various Raman active modes of the PU composite nanofibers. Compared with the pure PU nanofibers, noticeable structural changes and peak intensities were observed in PU composite nanofibers. This result indicates that the incorporated composite molecules were strongly bound with PU nanofibers to form the PU composite nanofiber structure. These results are in good agreement with that of FTIR data. Such kinds of composite structure are highly desirable when the application point of view is concerned.

Fig. 5 shows the TGA analyses of pristine PU and PU composite nanofibers. The TGA results showed that the pristine PU nanofibers decomposed in a single step. The onset of decomposition was found to be of $157, 195, 223, 267$ and $273\text{ }^{\circ}\text{C}$ corresponding to PU/R, PU/SR, PU/Ag, pristine PU and PU/C nanofibers, respectively. The thermal degradation behavior of pristine PU nanofibers is in good agreement with the previous reports [42,43]. However, the thermal degradation behaviors of composite PU nanofibers significantly differed from the pristine PU nanofibers. This is because the incorporated biological macromolecules significantly affected the composite nanofibers' thermal property. In other words, the incorporation of a biologically active group led to a loss of thermal stability compared to the pristine PU nanofibers. Furthermore, these results confirmed that the incorporated biological entities were evenly distributed on PU nanofibers. The thermal degradation of polymers at elevated temperatures is an inevitable event, and it completely relies on the constituent materials present in it. Therefore, the chemical reactions involved in thermal degradation of composite PU nanofibers led to property changes relative to the pristine PU nanofibers. This thermal degradation is generally attributed to the change of

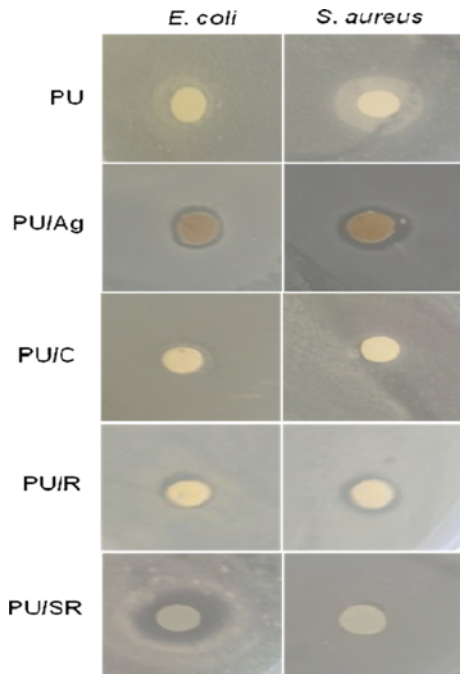


Fig. 6. Antimicrobial activities of pristine PU and PU composite nanofibers.

molecular weight of the polymer. As expected, the residual weight slightly differed with the addition of composite materials in the PU nanofibers. It is worth mentioning that the nature of composite materials introduced into nanofibers can significantly affect the residual amount in the composite nanofibers. It was found that the residual weight estimated at 900 °C was of 4, 10, 10.5, 13 and 15% corresponding to PU/R, PU/C, PU/SR, pristine PU and PU/Ag nanofibers, respectively. Therefore, the incorporation of biological entities into PU nanofibers remarkably lowers the thermal stability.

Fig. 6 shows the pristine PU and PU composite nanofibers which were cut into 6 mm diameter discs for the diffusion susceptibility test. The effect of antimicrobial activity of PU composite nanofibers in the culture media was studied by the disc diffusion susceptibility test, with MHA medium containing *S. aureus* and *E. coli* bacterial strains separately, after 24 h of incubation. The pristine PU nanofibers were used as the control sample. No bactericidal activity was detected for the pristine PU nanofibers, as shown in Fig. 6. However, more pronounced antimicrobial activity was observed for the PU composite nanofibers, and the zone diameter was shown in Table 1. The test was repeated and the results were found to be almost the same. The plates were checked for the prolonged incubation time to check the efficiency of the composite materials release.

In the case of composite nanofibers, more pronounced antimicrobial activity was observed because the composite material particles were attached to the periphery of the nanofibers by dip coating method. In other words, the composite materials were easily released to the media causing immediate bacterial cell death. This may be due to the fast growth of the cell when compared to the release of the particle from the polymer composite on the solid media. This is due to the easy release of the composite entities into media and the liquid-based media facilitating the ion transport in the presence of more water in the liquid media. Taking these features, we could expect the PU nanofibers containing composite materials would exhibit better antimicrobial activity. Systematic investigations among various pharmacological compounds have revealed that any drug may have the possibility of possessing diverse functions, and thus may have useful activity in completely different spheres of medicine. Therefore, the results clearly indicated the antibacterial activity of the utilized composite nanofibers and ascertained its value in the development of new antimicrobial products. Furthermore, the characteristics of the utilized composites, such as their sensing capability and antimicrobial properties, arise from their material surface and the beneficial properties of PU composite nanofibers.

CONCLUSIONS

We successfully obtained electrospun PU composite nanofibers by a simple dip coating method. The as-spun PU nanofibers were smooth with uniform diameters. The dip coating experimental results revealed that the composite materials can be uniformly coated on the electrospun PU nanofibers. The surface morphology, structure and thermal characterization of the synthesized composite nanofibers were studied by SEM, XRD, FT-IR, Raman and TGA analyses. From the disc diffusion test, the antimicrobial efficacy of the PU composite nanofibers was greater than that of pristine PU nanofibers. The PU composite nanofibers exhibited excellent antimicrobial property towards *S. aureus* and *E. coli* bacterial strains. Thus, the present study encourages the application of the electrospun rosin based fibers for biomedical applications such as prolonged wound dressing materials.

ACKNOWLEDGEMENTS

This research was financially supported by the Ministry of Education, Science Technology (MEST) and National Research Foundation of Korea (NRF) through the Human Resource Training Project for Regional Innovation (2012H1B8A2025931). This work was also supported by the National Research Foundation of Korea (NRF) grant funded by the Korea government (MEST) (No. 2012R1A2A2A01046086).

REFERENCES

1. A. Frenot and I. S. Chronakis, *Curr. Opin. Colloid Interf. Sci.*, **8**, 64 (2003).
2. N. Bhardwaj and S. C. Kundu, *Biotechnol. Adv.*, **28**, 325 (2010).
3. S. Agarwal, A. Greiner and J. H. Wendorff, *Prog. Polym. Sci.*, **38**, 963 (2013).

4. Z. M. Huang, Y. Z. Zhang, M. Kotaki and S. Ramakrishna, *Comp. Sci. Technol.*, **63**, 2223 (2003).
5. R. Gopal, S. Kaur, Z. Ma, C. Chan, S. Ramakrishna and T. Matsuura, *J. Membr. Sci.*, **281**, 581 (2006).
6. T. J. Sill and H. A. V. Recum, *Biomaterials*, **29**, 1989 (2008).
7. S. Agarwal, J. H. Wendorff and A. Greiner, *Polymer*, **49**, 5603 (2008).
8. R. Jayakumar, M. Prabaharan, P. T. Sudheesh Kumar, S. V. Nair and H. Tamura, *Biotechnol. Adv.*, **29**, 322 (2011).
9. A. Karchin, F. I. Simonovsky, B. D. Ratner and J. E. Sanders, *Acta Biomaterialia*, **7**, 3277 (2011).
10. R. Nirmala, H. M. Park, R. Navamathavan, H. S. Kang, M. H. El-Newehy and H. Y. Kim, *Mater. Sci. Eng. C*, **31**, 486 (2011).
11. D. H. Reneker and A. L. Yarin, *Polymer*, **49**, 2387 (2008).
12. J. H. He, Y. Wu and W. W. Zuo, *Polymer*, **46**, 12637 (2005).
13. M. M. Demir, I. Yilgor, E. Yilgor and B. Erman, *Polymer*, **43**, 3303 (2002).
14. U. Ojha, P. Kulkarni and R. Faust, *Polymer*, **50**, 3448 (2009).
15. S. Kidoaki, I. K. Kwon and T. Matsuda, *J. Biomed. Mater. Res. B Appl. Biomater.*, **76**, 219 (2006).
16. H. Deka, N. Karak, R. D. Kalita and A. K. Buragohain, *Polym. Degrad. Stab.*, **95**, 1509 (2010).
17. D. K. Chattopadhyaya and K. V. S. N. Raju, *Prog. Polym. Sci.*, **32**, 352 (2007).
18. X. Liu, Y. Zhao, Z. Liu, D. Wang, J. Wu and D. Xu, *J. Molecular Structure*, **892**, 200 (2008).
19. N. Fong, A. Simmons and L. A. P. Warren, *Acta Biomaterialia*, **6**, 2554 (2010).
20. R. Jayakumar, S. Nanjundan and M. Prabaharan, *React. Funct. Polym.*, **66**, 299 (2006).
21. I. Francolini, L. Dllario, E. Guaglianone, G. Doneli, A. Martinelli and A. Piozzi, *Acta Biomaterialia*, **6**, 3482 (2010).
22. S. H. Hsu, H. J. Tseng and Y. C. Lin, *Biomaterials*, **31**, 6796 (2010).
23. X. Liu, W. Xin and J. Zhang, *Bioresour. Technol.*, **101**, 2520 (2010).
24. P. A. Botham, D. Lees, H. P. A. Illing and T. Malmfors, *Regulatory Toxicology and Pharmacology*, **52**, 257 (2008).
25. S. V. Fulzele, P. M. Satturwar and A. K. Dorle, *Int. J. Pharm.*, **249**, 175 (2002).
26. P. M. Mandaogadea, P. M. Satturwara, S. V. Fulzele, B. B. Gogte and A. K. Dorle, *React. Funct. Polym.*, **50**, 233 (2002).
27. R. Nirmala, B. Woo-il, R. Navamathavan, D. Kalpana, Y. S. Lee and H. Y. Kim *Coll. Surf. B: Biointerfaces*, **104**, 262 (2013).
28. B. Woo-il, R. Nirmala, N. A. M. Barakat, M. H. El-Newehy, S. S. Al-Deyab and H. Y. Kim, *Appl. Surf. Sci.*, **258**, 1385 (2011).
29. H. B. Li, Y. Jiang and F. Chen, *J. Chromatogr. B*, **812**, 277 (2004).
30. L. L. Dong, Y. J. Fu, Y. G. Zu, M. Luo, W. Wang, C. Y. Li and P. S. Mu, *Food Chem.*, **133**, 430 (2012).
31. J. J. Liu, T. S. Huang, W. F. Cheng and F. J. Lu, *Int. J. Cancer*, **106**, 559 (2003).
32. B. Q. Li, T. Fu, Y. Yan, J. A. Mikovits, F. W. Ruscetti and J. M. Wang, *Biochem. Biophys. Res. Communun.*, **276**, 534 (2000).
33. R. Nirmala, D. Kalpana, J. W. Jeong, H. J. Oh, J. H. Lee, R. Navamathavan, Y. S. Lee and H. Y. Kim, *Colloids Surf., A: Physico-chem. Eng. Aspects*, **384**, 605 (2011).
34. R. Nirmala, J. H. Lee, R. Navamathavan, J. H. Yang and H. Y. Kim, *Mater. Lett.*, **65**, 2772 (2011).
35. J. Zhang, F. Zhang, Y. Luo and H. Yang, *Proc. Biochem.*, **41**, 730 (2006).
36. M. A. D. Nobile, A. Conte, C. Scrocco and I. Brescia, *Inno. Food Sci. Emerging Technol.*, **10**, 356 (2009).
37. Z. Jiang, K. J. Yuan, S. F. Li and W. K. Chow, *Spectroscopy Spectral Anal.*, **26**, 624 (2006).
38. R. Chen, C. Huang, Q. Ke, C. He, H. Wang and X. Mo, *Colloids Surf., B: Biointerfaces*, **79**, 315 (2010).
39. T. He, Z. Zhou, W. Xu, Y. Cao, Z. Shi and W. P. Pan, *Compos. Sci. Technol.*, **70**, 1469 (2010).
40. N. Barka, M. Abdennouri and M. E. L Makhfouk, *J. Taiwan Inst. Chem. Eng.*, **42**, 320 (2011).
41. S. Tunali, T. Akar, A. S. Ozcan, I. Kiran and A. Ozcan, *Sep. Purif. Technol.*, **47**, 105 (2006).
42. M. C. Saha, M. E. Kabir and S. Jeelani, *Mater. Sci. Eng. A*, **479**, 213 (2008).
43. F. A. Sheikh, M. A. Kanjwal, S. Saran, W. J. Chung and H. Kim, *Appl. Surf. Sci.*, **257**, 3020 (2011).